XANES identification of plutonium speciation in RFETS samples

V. LoPresti *, S.D. Conradson, D.L. Clark

Los Alamos National Laboratory, United States

Abstract

Using primarily X-ray absorption near edge spectroscopy (XANES) with standards run in tandem with samples, probable plutonium speciation was determined for 13 samples from contaminated soil, acid-splash or fire-deposition building interior surfaces, or asphalt pads from the Rocky Flats Environmental Technology Site (RFETS). Save for extreme oxidizing situations, all other samples were found to be of Pu(IV) speciation, supporting the supposition that such contamination is less likely to show mobility off site. EXAFS analysis conducted on two of the 13 samples supported the validity of the XANES features employed as determinants of the plutonium valence.
Published by Elsevier B.V.

Keywords: Actinide alloys and compounds; Oxide materials; Atomic scale structure; Electronic properties; EXAFS

At a cost of $7 billion, the Rocky Flats Environmental Technology Site (RFETS) – where plutonium (Pu)-trigger production for nuclear weapons occurred for nearly 40 years through 1989 – recently became the first DOE weapons complex site to undergo remediation and closure. Many areas at Rocky Flats had plutonium contaminated soil and water due to the improper disposal of contaminated materials, ruptured or leaking pipes, fires, or faulty storage units. By far, the largest source of plutonium contamination in soils resulted from a drum storage area known as the 903 Pad, where leaking drums contaminated the soils with approximately 86 g (5.3 Ci) of plutonium, and wind and water erosion carried plutonium and americium in a well-defined pattern to the east and southeast, beyond the eastern site boundary in some cases. The Environmental Protection Agency designated the RFETS a Superfund cleanup site, and in March 1995, DOE estimated the cleanup for Rocky Flats would cost in excess of $37 billion and take 70 years to complete. However, the formation of an Actinide Migration Evaluation advisory group in 1995 led to the development of actinide transport models that facilitated the integrated scientific understanding necessary to reach agreement regarding target cleanup levels and to expeditiously proceed with site cleanup and remediation. In this study, XANES was used to determine plutonium valence in soil and concrete samples from RFETS. This study supports the scientific understanding that helped focus site-directed efforts, which aided the DOE in closing RFETS in December 2005, one year ahead of schedule [1–3].

1. Samples/methods

In a more-global study, a total of 13 RFETS samples were analyzed, however, in this poster, we reported only on sample groups in which at least one sample of the group was adequate for EXAFS analysis subsequent to XANES.

XAFS measurements on RFETS samples were performed over a period of almost five years, utilizing two different beamlines. Hence, all runs included Pu standards so that the RFETS samples could be directly compared with the spectra of known compounds measured under identical beamline and detector conditions to improve the reliability of XANES measurements by eliminating the possibility of beamline configuration-induced artifacts. These usually included both a Pu(IV) and a Pu(VI) standard, with the former a calcined PuO_2 sample that we now know would have actually been $PuO_{2-+x-y}(OH)_{2y} \cdot z(H_2O)$ [4] and the latter a freshly prepared PuO_2^{2+}-hydroxycarbonate, whose stoichiometry varied somewhat among different runs. Spectra of standards and RFETS samples from a given run were analyzed identically and the RFETS XANES interpreted by direct comparison with the data from the standards.

---

* Corresponding author.
 E-mail address: vcl@lanl.gov (V. LoPresti).

2. Experimental and analytical procedures

2.1. RFETS samples, Pu L_{II} edge XANES and EXAFS

Because of the extremely small amount of Pu in most samples, a much longer total acquisition time – up to 60 s for each point in a spectrum prepared by averaging up to five individual scans – was often required to obtain interpretable XANES spectra, which, even so, are often noisy. XAFS measurements were performed on end stations 4-2 and 11-2 of the Stanford Synchrotron Radiation Laboratory, under dedicated synchrotron X-ray production conditions (3.0 GeV e⁻, 45–100 mA).

Second-order polynomials were fit through both pre- and post-edge regions for longer, more-complete scans; linear fits were used for noisier data. Spectra were offset and scaled so that the edge jump spans the range zero to unity so that all results can be compared directly on a per-atom basis. Multiple scans were averaged after interpolating the data of the individual scans to match the energies for the longest scan. Peak and inflection point energies, with the latter referred to as the "edge" energy, were defined as the zero crossings of, respectively, the first and second derivatives. For the samples "fire deposition, concrete" and "soil sample B" (Pad 903), Extended X-ray Absorbance Fine Structure (EXAFS) was separated from spectra by approximating the smooth, atomic background with a polynomial spline, with knot positions adjusted to minimize the area of the modulus of the Fourier transform of the k^3-weighted EXAFS below $R = 1.0$ Å. Fourier transforms were always performed after the application of a sine window function to the EXAFS. Metrical parameters were obtained from the EXAFS via nonlinear, least-squares, k-space, k^3-weighted curve-fits using the standard, harmonic EXAFS equation summed over shells and amplitudes and phases obtained from code FEFF7. The emphasis in curve-fits was to identify the existence of distinct neighbor shells, not on quantifying numbers of atoms or distribution widths. To assess confidence level in these assignments, the phase of the data was compared with the fit for each shell in k and R [5,6].

3. Results and discussion

3.1. Pad 903 soils (Figs. 1 and 3a)

Cumulatively, the XANES data (Fig. 1) indicate that all Pad 903 soil samples are of predominately (IV) speciation, a conclusion supported by the EXAFS data for Sample B that indicate a
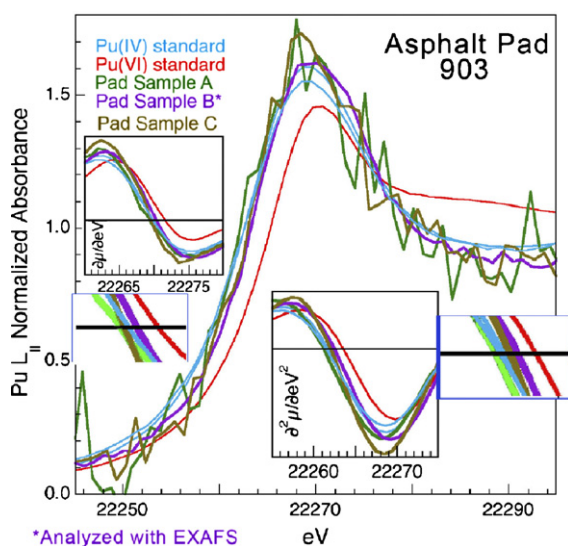

Fig. 1. XANES of three pad 903 soil samples with Pu(IV) and Pu(VI) standards. Insets show first derivative (peak position) with magnification of zero-crossing (left) and second-derivative (inflection point) with magnification of zero-crossing (lower right).
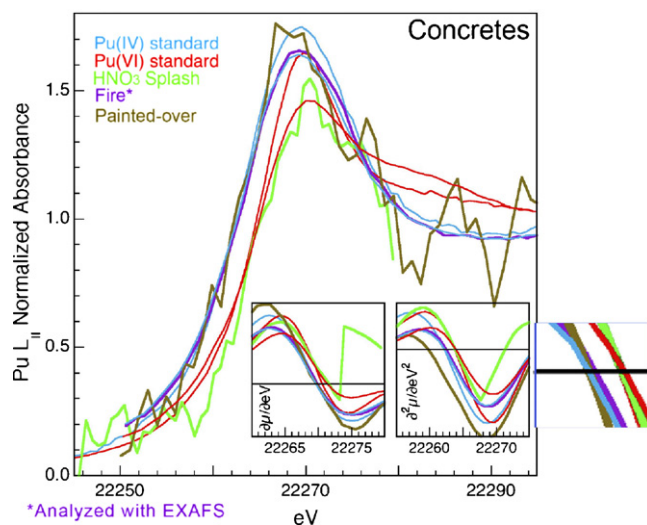

Fig. 2. XANES of three concrete samples with Pu(IV) and Pu(VI) standards. Insets show first derivative (peak position) (lower left) and second-derivative (inflection point) with magnification of zero-crossing (lower right).

PuO₂-like pattern of Pu–O and Pu–Pu shells, thereby supporting the criteria used in the XANES-based assessment.

3.2. Concretes (Figs. 2 and 3)

Cumulatively, the XANES data (Fig. 2) indicate that the fire deposition and painted-over concrete samples are of predominately (IV) speciation, a conclusion supported by the EXAFS data for the fire-deposition samples (Fig. 3), that indicate a PuO₂-like pattern of Pu–O and Pu–Pu shells. By contrast, deposited onto an internal concrete floor surface from a PUREX separations line utilizing concentrated nitric acid, the XANES spectrum of the HNO₃ splash sample is illustrative of Pu(VI) speciation (Fig. 2). Two standards of each type are included since these three concrete spectra were obtained in two separate runs. Because the measurement of a single spectrum takes a few hours, the probability of a loss of beam that terminates that spectrum is high and the individual spectra from a particular sample that will be averaged to give the final spectrum will vary in length. In this case we calculated two such spectra, one using fewer scans that progressed to higher energy and one with more scans and less noise that is presented here. Normalization of the latter was confirmed by comparison with the former. Analysis of the energies of the XANES features was performed on the latter.

More quantitative characterization of the local ordering of the Pu–O/Pu shells is obtained from the metrical results calculated by the EXAFS curve-fits (Table 1). These fits utilizing the PuO₂ structure as an organizing metric for the numbers and types of neighbor shells exhibit very good (Fire Concrete) to fair (Pad Sample B with high noise levels) correspondence between data and fit, demonstrating that the assignment of both samples to this class of compounds is correct. The correspondence between both moduli and real components of the fits and the data clearly establish the origin of the features as O at lower R and Pu for the higher-R feature. Only Pu–O/Pu distances are reported because
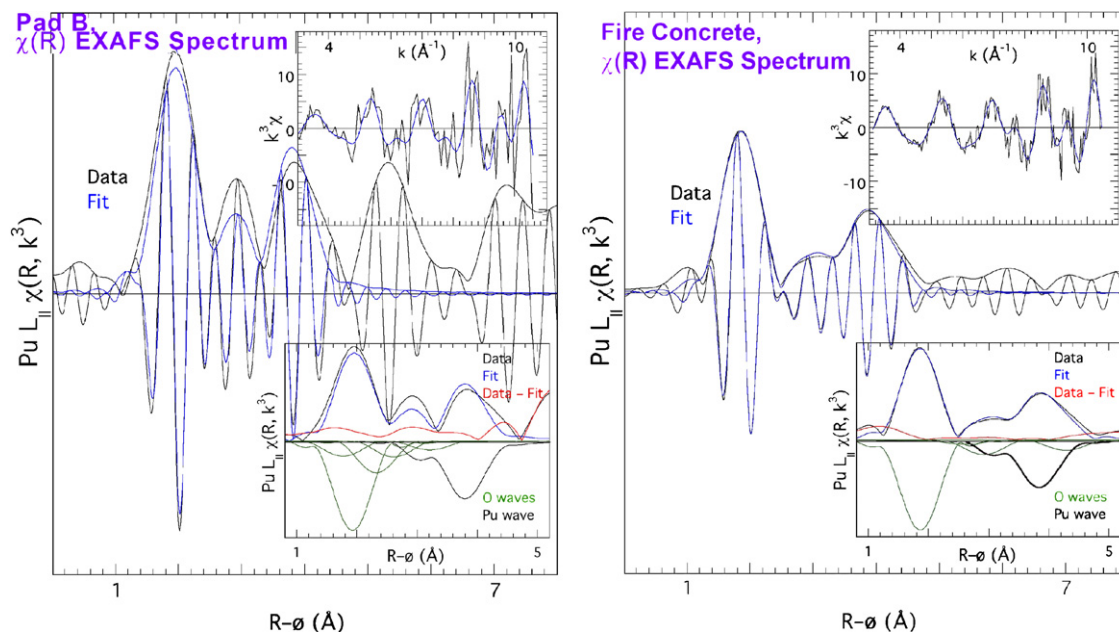
Fig. 3. EXAFS of Pad 903 soil sample B and fire-deposition concrete sample. The insets show the $\chi(k)$ representation (upper) and the components of the fit (lower), including the difference between the data and the fit (red) and (inverted) the moduli of the individual Pu–O (green) and Pu–Pu (black) contributions.

correlation between the numbers of atoms and the Debye-Waller factors is exacerbated by the short extent of the data and the noise level. Complete EXAFS parameters are shown in Table 2.

This similarity confirms the identification of these samples as conforming to the speciation found in this class of materials, with a greater departure from the crystallographic structure because of hydration displayed by the sample that derived from an out-

Table 1
Radial Pu–O/Pu distances for Pu(IV) compounds

Sample	O < 1.95	O at 2.2	O at 2.34	O at 2.8	O at 3.0	O at 3.25	O at 3.5	O at 4.47	Pu
PuO$_2$*			2.34					4.47	3.82
PuO$_2$			2.35					4.53	3.84
PuO$_2$ standard			2.33					4.48	3.85
Fire Concrete			2.32		3.05		3.38	4.62	3.84
Pad Sample B			2.38	2.74	3.0		3.65	†	3.83

Pu–O/PU shells obtained from the metrical results calculated by the EXAFS curve-fits; (*) Crystallographic structure; (†) feature in spectrum but extra shell not included in fit; blank field – no evidence for presence of shell.

Table 2
Complete EXAFS parameters

	R	*N*	Sigma	DE0
Fire concrete sample				
O	2.32 ± 0.02	6.3 ± 1.8	0.070 ± 0.020	5.4 ± 4.5
O	3.05 ± 0.03	0.9 ± 0.4	0.099 ± 0.022	6
O	3.38 ± 0.02	2.4 ± 0.8	0.075	3.6 ± 2.5
Pu	3.82 ± 0.02	4.1 ± 1.2	0.040 ± 0.04	8.2 ± 2.5
O	4.62 ± 0.02	2.5 ± 0.8	0.064 ± 0.02	12.1 ± 1.5
PadB soil sample				
O	2.21 ± 0.03	0.8 ± 0.5	0.05	9
O	2.37 ± 0.02	5.6 ± 1.4	0.060 ± 0.016	8.5 ± 3.8
O	2.75 ± 0.02	2.2 ± 0.9	0.040 ± 0.016	9.5 ± 3.8
O	3.02 ± 0.02	1.3 ± 0.7	0.040 ± 0.013	9.5 ± 3.7
O	3.61 ± 0.02	1.1 ± 0.2	0.040 ± 0.013	9.5 ± 4.0
Pu	3.81 ± 0.02	4.8 ± 1.5	0.04	8

No uncertainty means the parameter was not allowed to float in the fit. Many of the parameters were constrained with respect to others, i.e., they could only vary from usually the primary O shell by a limited amount.
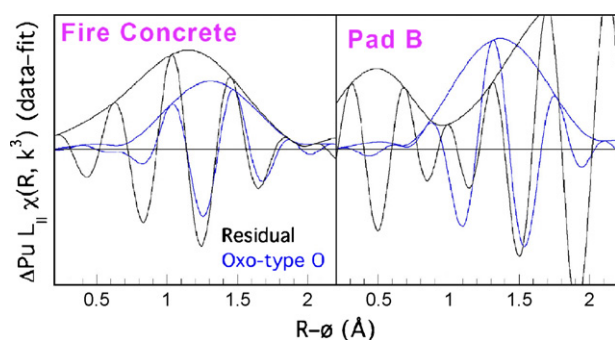
Fig. 4. Fourier transform moduli of EXAFS of RFETS concrete fire-deposition (left) and 903 pad sample B (right) residuals fit with oxo-type O shell.

door rather than an indoor location, and which had possibly been deposited from multiple events rather than a single one.

The remaining issue in the speciation is the recent finding that oxidation of PuO_2 to $PuO_{2.25}$ proceeds via the formation of Pu(V)-oxo moieties[7,8]. This evidence for mixed valence is best found by identifying the signature of the oxo group in the EXAFS as a component around $R = 1.3$ Å that is well fit by an O shell at a Pu–O distance at 1.8–1.9 Å. This contribution is isolated by subtracting from the data a fit containing the waves from all of the near neighbors except this one, which can then be fit separately to establish the correspondence between any residual remaining after subtraction and a Pu–O wave (Fig. 4). Although this residual from the spectrum of the Fire Concrete sample is not completely fit by the contribution from an O shell, the real components of the data and fit align well and the modulus of the fit is contained within the data and matches it on the high-R side. The Pu–O distance of 1.77 Å is close enough to that expected to corroborate that this sample, consistent with exposure to elevated temperature that promotes oxidation (although additional ambient temperature processes have been observed), is potentially superstoichiometric. In contrast, the contribution of the O shell at 1.83 Å that is the best fit to this much larger residual for the spectrum from Pad Sample B is not associated with any particular feature and does not correspond to the data. It is therefore unlikely that it has been subjected to any significant degree of oxidation [9].

The available EXAFS spectra therefore provide convincing evidence in support of the conclusion that the Pu in both the RFETS sample 7 (concrete) and sample 11 (pad) is not only Pu(IV) but also resides in a PuO_2-type of compound. This confirmatory analysis provides an additional degree of confidence in the conclusions about Pu speciation derived solely from XANES, affirming that the XANES criteria used to assess speciation of the other samples are largely valid.

Acknowledgements

References

[1] D.L. Clark, D.R. Janecky, L.J. Lane, Phys. Today (2006) 34.
[2] Kaiser-Hill, Actinide migration evaluation pathway analysis summary report. Kaiser-Hill Company 2002 ER-108 p. 30.
[3] R.T. Hurr, Hydrology of a Nuclear-processing plant site, Rocky Flats. U.S. Geological Survey, 1976, Open File Report 76–268.
[4] S.D. Conradson, B.D. Begg, D.L. Clark, C. den Auwer, M. Ding, P.K. Dorhout, F.J. Espinosa-Faller, P.L. Gordon, R.G. Haire, N.J. Hess, R.F. Hess, D.W. Keogh, L. Morales, A.J. Lupinetti, L.A. Morales, M.P. Neu, P.D. Palmer, P. Paviet-Hartmann, W.H. Runde, C.D. Tait, D.K. Veirs, P.M. Villella, J. Am. Chem. Soc. 126 (41) (2004) 13443.
[5] B.D. Begg, E.R. Vance, S.D. Conradson, J. Alloys Compd. 271 (1998) 221.
[6] E.R. Vance, R.A. Day, M. Hambley, S.D. Conradson, in: W.J. Gray, I.R. Triay (Eds.), Scientific Basis for Nuclear Waste Management XX, Mater. Res. Soc., Warrendale, PA, 1997, p. 325.
[7] S.D. Conradson, B.D. Begg, D.L. Clark, C. Den Auwer, F.J. Espinosa-Faller, P.L. Gordon, N.J. Hess, R. Hess, D.W. Keogh, L.A. Morales, M.P. Neu, W. Runde, C.D. Tait, D.K. Veirs, P.M. Villela, Inorg. Chem. 42 (12) (2003) 3715.
[8] J.M. Haschke, T.H. Allen, L.A. Morales, Science 287 (5451) (2000) 285.
[9] J.L. Stakebake, D.T. Larson, J.M. Haschke, J. Alloys Compd. 202 (1993) 251.